Journal of Photochemistry, 6 (1976/77) 405 - 430
© Elsevier Sequoia S.A., Lausanne — Printed in Switzerland

THE PHOTOLYSIS OF SULFUR DIOXIDE IN THE PRESENCE OF FOREIGN GASES: IX. ALLENE

KENNETH PARTYMILLER, JAMES F. MEAGHER* and JULIAN HEICKLEN

Department of Chemistry and Center for Air Environment Studies, The Pennsylvania State University, University Park, Pa 16802 (U.S.A.)

(Received July 8, 1976; in revised form November 1, 1976)

Summary

SO_2 was photoexcited at 25 °C and 313.0 nm in the presence of allene. The quantum yields of the gas phase products, C_2H_4 and CO, were determined over a wide range of allene and SO_2 pressures as well as in the presence of CO_2, NO, and H_2O. The quantum yield of C_2H_4, $\Phi\{C_2H_4\}$, increases with the ratio [allene]/[SO_2] to a maximum value of 13.1×10^{-3}. In the presence of excess CO_2, NO, or H_2O, or at higher allene pressures, $\Phi\{C_2H_4\}$ is reduced for any [allene]/[SO_2] ratio. At higher [allene]/[SO_2] ratios NO is a much less efficient quencher than at low ratios and thus both singlet and triplet states of SO_2 must participate in C_2H_4 production. The quantum yield of CO, $\Phi\{CO\}$, also increases with the ratio of [allene]/[SO_2] to a maximum value of 20.9×10^{-3}. At low values of the ratio [allene]/[SO_2] as well as low total pressure, $\Phi\{CO\}$ is quenched initially by adding CO_2, NO, and H_2O in a manner similar to $\Phi\{C_2H_4\}$. For continued increases in the pressures of CO_2, NO, and H_2O or at higher values of [allene]/[SO_2], $\Phi\{CO\}$ is enhanced. Both the singlet and triplet emitting states, as well as a previously proposed non-emitting triplet state are necessary to interpret the photochemistry of SO_2 in this study. A relatively complete mechanism is proposed, all of the pertinent rate coefficient ratios are derived and tabulated, and from these values $\Phi\{C_2H_4\}$ and $\Phi\{CO\}$ values are computed which agree well with the observed values.

Introduction

The reactions of electronically excited sulfur dioxide molecules are of interest theoretically as well as practically in understanding the role of this

---

CAES Report No. 426-76.

*Present address: Tennessee Valley Authority, Air Quality Branch, Muscle Shoals, Alabama 35660 (U.S.A.).

molecule in atmospheric chemical reactions. Although SO_2 is a structurally simple molecule, its primary photophysical processes are not clearly established. As radiation above 218 nm is of insufficient energy to rupture the S–O bond, any photochemically induced reactions of SO_2 in the atmosphere are the result of interactions with bound excited states of the molecule. Both singlet and triplet states participate in its photochemistry upon absorption of ultra-violet radiation of wavelengths present in the atmosphere. These electronically excited states of SO_2 are of current interest because of their possible role in the removal of SO_2 from polluted atmospheres. Olefinic hydrocarbons may enhance the formation of aerosols in SO_2 polluted atmospheres.

Two emitting states of SO_2, a singlet designated $SO_2(^1B_1)$ and a triplet designated $SO_2(^3B_1)$ have been observed upon excitation into the region from 250 to 340 nm. The simplest interpretation of this fact is that the initial absorption is the $SO_2(^1B_1) \leftarrow SO_2(\tilde{X}, {}^1A_1)$ transition, and that $SO_2(^3B_1)$ is produced by intersystem crossing. Most of the early studies of the photophysical properties of SO_2 were done in this region via emission lifetime measurements, and fluorescence and phosphorescence studies [1 - 10].

Excited SO_2 has been shown to be chemically reactive upon excitation into the second absorption band (250 - 340 nm) [11 - 18] as well as the first absorption band (350 - 390 nm) [19 - 26]. Quenching reactions of $SO_2(^1B_1)$ and $SO_2(^3B_1)$ have been studied using a variety of quenching gases and reaction conditions [4, 10, 18, 27].

Past work in this laboratory [18, 28 - 31] and elsewhere [11 - 14, 17, 32 - 36] with photoexcited SO_2 has not been consistent with a mechanism including only the two emitting states. The fluorescence quantum yields do not obey Stern–Volmer quenching and thus there is evidence that $SO_2(^1B_1)$ is not the state formed initially upon absorption [37]. Participation of a non-emitting singlet state, SO_2^*, and one or two non-emitting triplet states, SO_2^{**} and $SO_2^{\ddagger}$, have been included in the various mechanisms to explain the data [18, 26, 28 - 31, 37 - 39].

The present study involves the photolysis of SO_2 at 313.0 nm in the presence of allene and various quenching gases. Previous studies by Luria *et al.* [38, 39] show CO, C_2H_4, and an aerosol to be the major reaction products. It is believed that the quantum yield of C_2H_4 as well as CO will serve as a measure of the participation of the various possible reactive states and that the addition of quenching gases will permit the further characterization of these states.

Experimental

Photolysis was carried out in an opaque cylindrical cell of dimensions 50 cm × 5.0 cm o.d. which had quartz windows bonded to both ends. A 6 mm o.d. perforated tube passed down the length of the cell to insure thorough mixing when the gases were introduced through it. The radiation source was a Hanovia 140 W medium pressure, U-shaped, type SH, mercury arc. The radiation was collimated by a quartz lens and passed through a Corning 7-54 (type 9863) glass filter and an Ealing 313.0 nm interference filter before entering the cell through the quartz window. In later experiments where low quantum yields were expected an identical radiation source was placed at the opposite end of the cell to double the intensity. A General Electric 935 photodiode was, alternatively, placed at the opposite end of the cell to measure light intensity.

All work was carried out in a high vacuum line using Teflon stopcocks with Viton "O" rings. Pressures from 20 to 750 Torr were measured on 0 - 50 Torr or 0 - 800 Torr Wallace and Tiernan absolute pressure gauges. A silicone oil manometer was employed for most pressure measurements below 20 Torr. Pressures of less than 0.8 Torr were achieved by expansion.

Allene was supplied by Linde/Union Carbide. It was purified first by passing through a gas chromatograph with a 30 ft. column of dimethyl sulfolane and then distilled three times from —112 °C to —196 °C. All other gases were supplied by Matheson Gas Products. Sulfur dioxide (anhydrous) was distilled once from —95 °C to —130 °C and stored in an opaque storage bulb. Nitric oxide was passed through silica gel and then distilled from —186 °C to —196 °C. It was also stored in an opaque storage bulb. Gas chromatographic analysis showed only a small nitrogen impurity. Carbon dioxide (bone dry) was distilled from —130 °C to —196 °C. Water (triple distilled and deionized) was repeatedly degassed at —196 °C. Azomethane was prepared according to the procedure given by Renaud and Leitch [40]. It was then purified by distillation from —90 °C to —130 °C and stored in an opaque storage bulb. All of the above gases were degassed at —196 °C immediately before use.

After irradiation, the vapor phase products were analyzed by gas chromatography. Ethylene was analyzed by expansion of an aliquot of the reaction mixture into an injection loop attached to a Varian model 1200 gas chromatograph. The mixture was separated by a 6 ft. × ¼ in. o.d. stainless steel column packed with 60/80 mesh Chromosorb 101 maintained at 100 °C and with a flow rate of 30 cm^3/min of helium. The ethylene and allene were then detected by a flame ionization detector maintained at 150 °C. The detector response of ethylene relative to allene was calibrated and thus the unreacted allene (always greater than 99% of the initial amount) was used as an internal standard to determine the amount of ethylene present. Carbon monoxide was analyzed by first allowing the reaction mixture to expand into two spiral traps maintained at liquid nitrogen temperature and then pumping the non-condensable carbon monoxide, by means of a Toepler pump, into a second gas chromatograph injection loop. In experiments where nitric oxide was present, a trap cooled in solid nitrogen was used in place of the second spiral trap to condense the nitric oxide. The carbon monoxide was then injected into a Gow Mac model 40-05D gas chromatograph using a thermistor detector maintained at 0 °C. A 6 ft. × ¼ in. o.d. copper column packed with Linde 13X molecular sieves, maintained at 25 °C with a flow rate of 70 cm^3/min of helium provided separation of the non-condensable gases. This system was calibrated with standard samples of carbon monoxide and blanks were performed with all of the gases used. In later experiments the carbon monoxide was converted to methane by means of a nickel catalyst by the method of Williams *et al.* [41]. The methane was then detected with greater sensitivity by the Varian model 1200 flame ionization detector gas chromatograph as previously described. This system was also calibrated with standard samples of CO, C_2H_4, and allene and thus allowed a single injection method to detect, with allene again acting as an internal standard, both carbon monoxide and ethylene.

Azomethane was used as the actinometer in this study. The quantum yield of azomethane for N_2 production is unity at 313.0 nm. The N_2 produced in the azomethane photolysis was determined in the same manner as described above using the Gow Mac thermistor detector gas chromatograph with the same column and detectors. The gas chromatograph was calibrated for N_2 using standard samples. The General Electric 935 photodiode was used to match absorbances of SO_2 and azomethane. The amount of carbon monoxide and ethylene produced in each experiment was determined and converted to quantum yields by knowledge of the N_2 yield obtained from azomethane photolysis at equal absorbances.

Results

Photolysis of SO_2 in the presence of allene and at times CO_2, NO, and/or H_2O was performed at 25 °C with radiation of 313.0 nm. An SO_2 pressure of 2.7 Torr reduced the intensity of radiation reaching the photodiode by approximately 50%.

Carbon monoxide and ethylene analyses were performed for identical experiments with varying photolysis times. In these experiments product growth as a function of time was linear and showed no detectable induction period as well as no fall off at longer photolysis times. Mixtures allowed to stand overnight gave no products. This indicates that the carbon monoxide and ethylene were primary products and that there was not a significant amount of light scattering from the aerosol under the experimental conditions employed.

A series of experiments were performed at an SO_2 pressure of 4.28 ± 0.10 Torr and at an allene pressure of 4.29 ± 0.10 Torr in which the incident radiation intensity, I_a, was varied from 0.58 to 7.7 mTorr/min. There was no systematic variation in the results which were found to be identical within experimental scatter. For most of the experiments performed in this study, I_a was between the above limits. For a few experiments with low SO_2 pressures, I_a was as small as 0.03 mTorr/min.

In the following series of experiments either the $[SO_2]$ was held constant at pressures of 0.97 ± 0.10 Torr, 2.05 ± 0.10 Torr, 2.50 ± 0.10 Torr and 5.9 ± 0.2 Torr and the allene pressure varied in the range of 14.3 mTorr

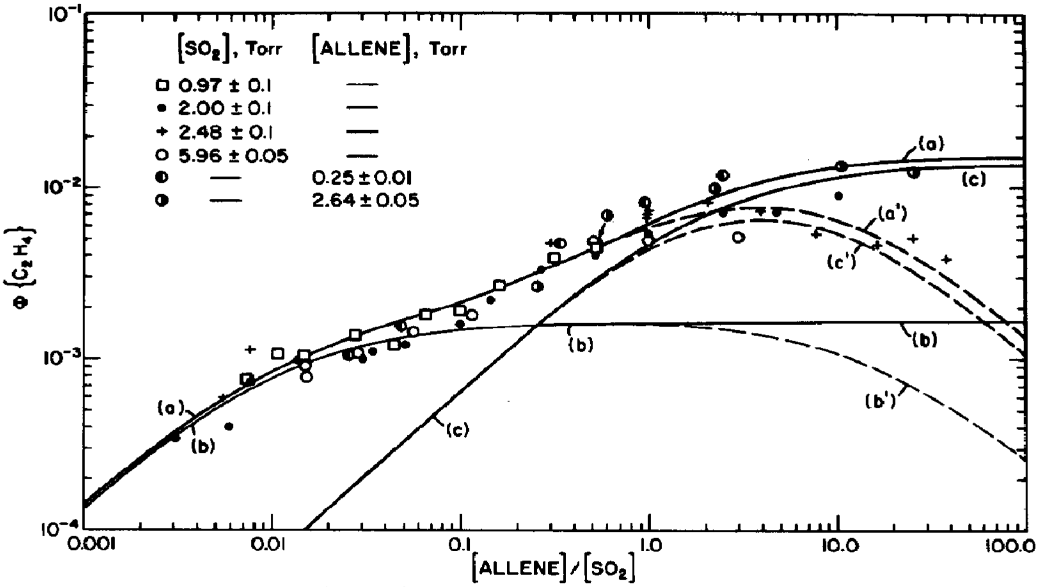

Fig. 1. Log–log plot of $\Phi\{C_2H_4\}$ *vs.* [allene]/[SO_2]. Four sets of data points are for constant [SO_2] and variable [allene], whereas two sets of data points are for variable [SO_2] and constant [allene]. The curves are theoretically computed from the rate coefficients listed in Table 1. (a) and (a′), total $\Phi\{C_2H_4\}$; (b) and (b′), $\Phi^3\{C_2H_4\}$; (c) and (c′), $\Phi^1\{C_2H_4\}$; (a) (b) and (c) are for [allene] = 1.0 Torr; (a′) (b′) and (c′) are for [SO_2] = 2.7 Torr.

to 95.3 Torr, or the allene pressures were held constant at 0.250 ± 0.010 Torr and 2.64 ± 0.05 Torr, and the SO_2 pressure was varied from 0.1 Torr to 15.6 Torr. $\Phi\{C_2H_4\}$ was found to be dependent only upon the ratio of [allene]/[SO_2] at values of this ratio of less than 1.0 (Fig. 1). At higher values of this ratio, $\Phi\{C_2H_4\}$ was found to be dependent upon [allene], with little, if any, dependence on [SO_2]. $\Phi\{CO\}$ values were found to be dependent only upon the ratio [allene]/[SO_2] at low allene pressures. $\Phi\{CO\}$ increased slightly with increases in the ratio and was always greater than $\Phi\{C_2H_4\}$ in each run, but not by a constant multiple. At high allene pressures $\Phi\{CO\}$ had a complex dependence on [SO_2] and [allene] (Figs. 2 - 6). These results agree qualitatively with the very limited data of Luria and Heicklen [38] though their absolute values for $\Phi\{CO\}$ were slightly higher than ours. Their values for $\Phi\{C_2H_4\}$ were found to be identical with ours within the scatter of the experimental data.

We performed two series of experiments by adding various amounts of CO_2 to mixtures in which [SO_2] equalled 2.63 ± 0.09 Torr and [allene] equalled 0.251 ± 0.010 or 2.65 ± 0.12 Torr. $\Phi\{C_2H_4\}$ decreased as [CO_2] was raised. $\Phi\{C_2H_4\}$ was found to be half quenched at a CO_2 pressure of approximately 7.0 Torr for both ratios of [allene]/[SO_2] (Figs. 7 and 8). $\Phi\{CO\}$ was found to decrease at both [allene]/[SO_2] ratios with increasing [CO_2] to a minimum value at 30 Torr of CO_2 for the lower ratio and at 125 Torr of CO_2 for the higher [allene]/[SO_2] ratio. With the addition of greater amounts of CO_2, $\Phi\{CO\}$ increased slightly and then leveled off (Figs. 9 and 10).

Luria and Heicklen [38] previously reported a reduction in Φ {CO} when 750 Torr of CO_2 were added to a mixture of 2.2 Torr of SO_2 and 2.2 Torr of allene. Two series of experiments were performed in the presence of ~600 Torr of CO_2. SO_2 pressures were held at 2.66 ± 0.08 Torr and 5.28 ± 0.15 Torr while allene was varied from 23.2 mTorr to 19.7 Torr and from 34.4 mTorr to 10.8 Torr respectively. With ~600 Torr of CO_2 present, Φ {C_2H_4} was completely quenched. Φ {CO} increased with increasing allene pressure

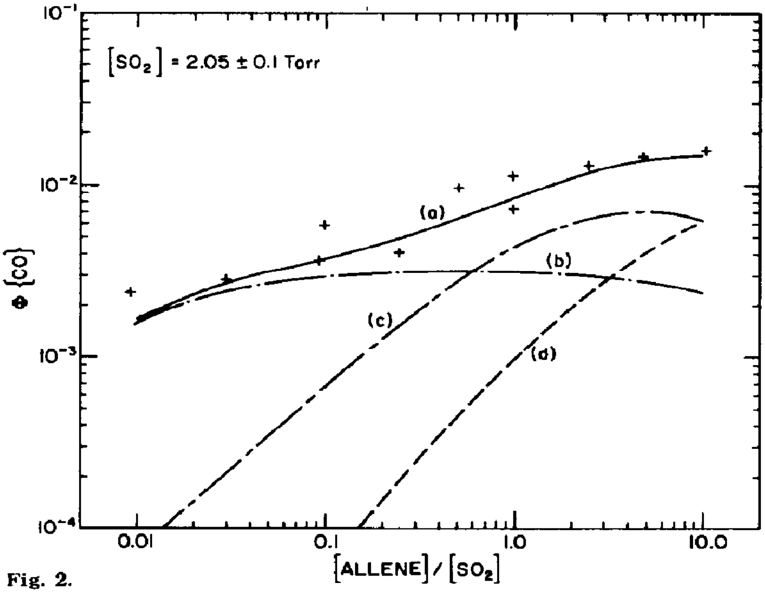

Fig. 2.

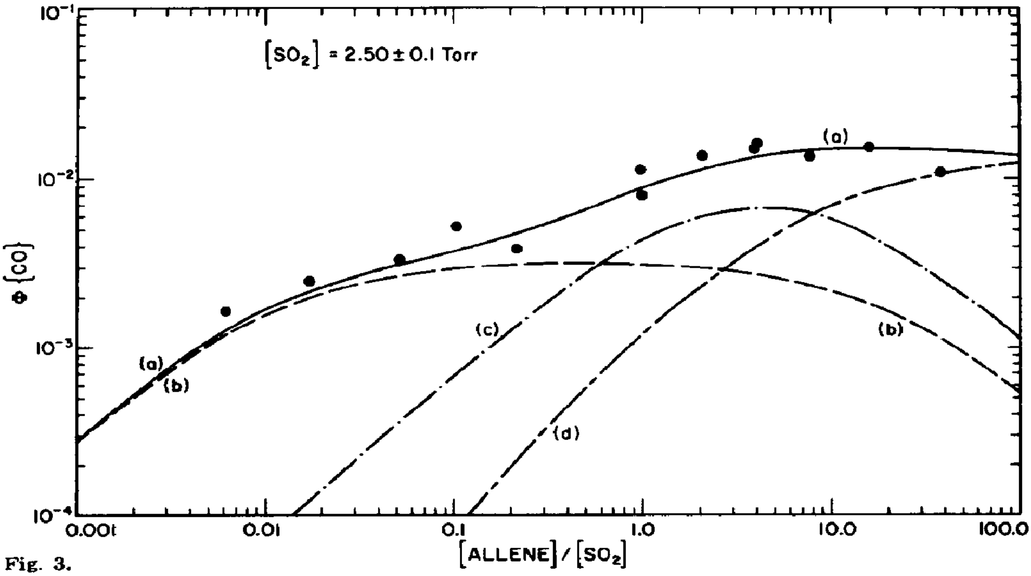

Fig. 3.

(For captions see page 412.)

to a plateau value of ~6 × 10^{-3} at approximately 10 Torr of allene (Fig. 11) and was found to have a similar value in this region to that of Luria and Heicklen.

Three series of experiments were performed by adding NO as a quenching gas to the reaction mixture. In these experiments the SO_2 pressure was 2.70 ± 0.12 Torr throughout. In the first series the allene pressure was 0.253 ± 0.007 Torr and the NO pressure varied from 31.3 mTorr to 3.0 Torr. In the second the allene pressure was 2.68 ± 0.07 Torr and the NO

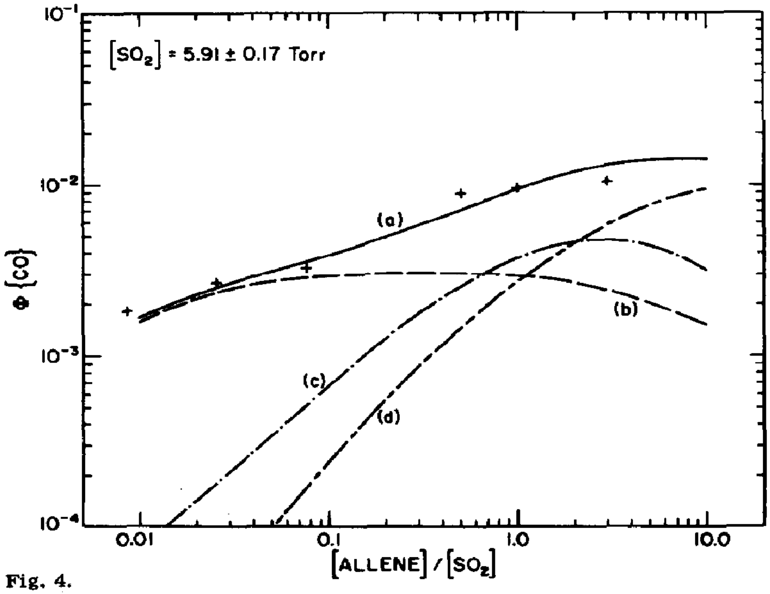

Fig. 4.

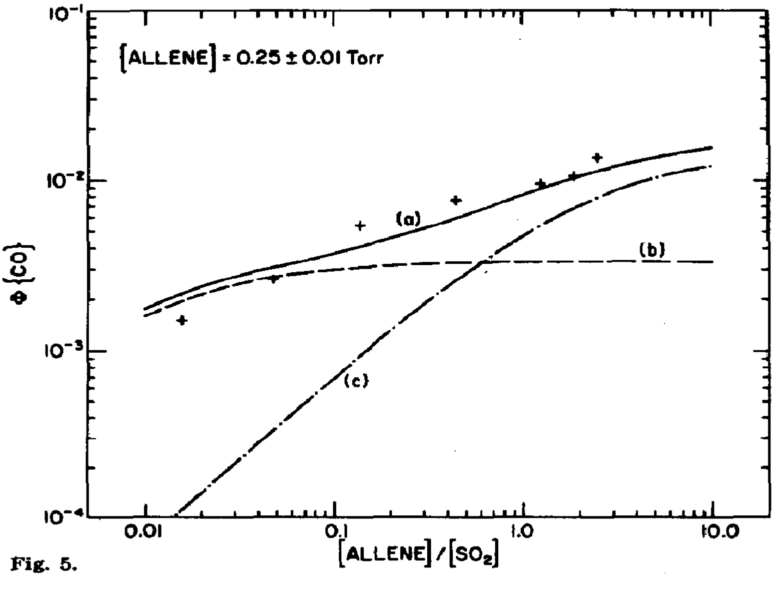

Fig. 5.

(For captions see page 412.)

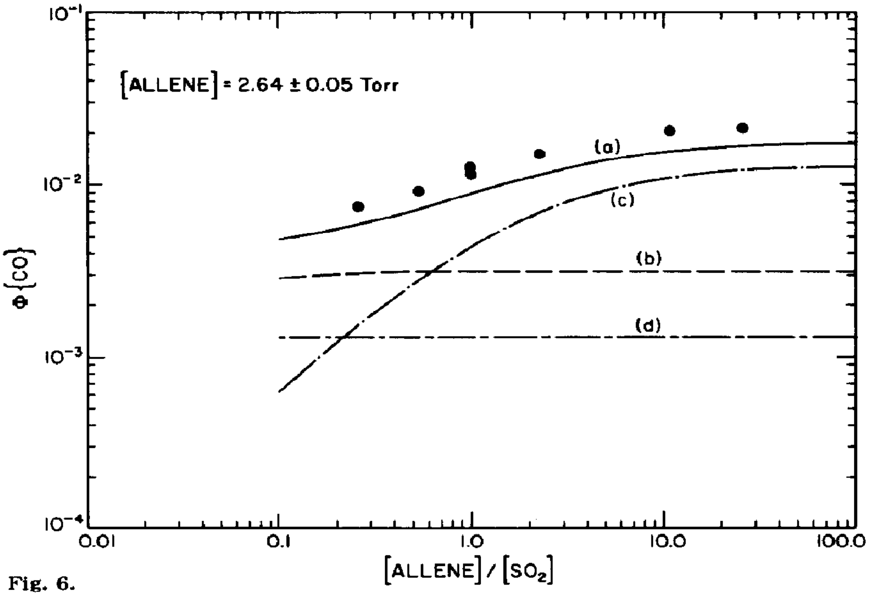

Fig. 6.

Figs. 2 - 6. Log–log plot of $\Phi\{CO\}$ *vs.* [allene]/[SO_2]. The curves are theoretically computed from the rate coefficients used in Table 1. (a), total $\Phi\{CO\}$; (b), $\Phi^3\{CO\}$; (c), $\Phi^1\{CO\}$; (d), $\Phi^{**}\{CO\}$.

pressure was varied from 2.44 mTorr to 97.5 Torr. In the third the allene pressure was 23.5 ± 0.5 Torr and the NO pressure was varied from 10.4 mTorr to 100 Torr. In all cases $\Phi\{C_2H_4\}$ and $\Phi\{CO\}$ were quenched very effectively. Both were half quenched at pressures of approximately 1.2, 4.0, and 25 Torr of NO, respectively, for the three series (Figs. 12 - 17).

Four series of experiments were performed by adding various pressures of H_2O as a quenching gas to the reaction mixture. In the first three of these series the SO_2 pressure was 2.70 ± 0.12 Torr and these three series were run at allene pressures of 0.252 ± 0.003 Torr, 2.66 ± 0.12 Torr, and 25.0 ± 0.10 Torr. H_2O was varied from approximately 1.0 to 18 Torr for all of these experiments. For the two series performed with lower allene pressures, $\Phi\{C_2H_4\}$ was half-quenched at H_2O pressures of approximately 4.0 Torr (Figs. 18 and 19). In the series with 25.0 Torr of allene, $\Phi\{C_2H_4\}$ was reduced very slightly by the addition of up to 18 Torr of H_2O (Fig. 20). The addition of up to 18 Torr of water reduced $\Phi\{CO\}$ by 40, 45, and 20% respectively for these three series (Figs. 21 - 23). These data again agree qualitatively with that of Luria and Heicklen [38].

In the fourth series of quenching experiments with H_2O, the pressure of SO_2 was 0.95 ± 0.06 Torr and that of allene was 0.104 ± 0.002 Torr. H_2O was again varied from about 1.0 to 18 Torr. In these experiments only $\Phi\{C_2H_4\}$ was measured and it was found to decrease with increasing H_2O pressure to a 50% value at approximately 3 Torr of H_2O (Fig. 24).

The quenching studies described above using NO and H_2O were repeated in the presence of ~600 Torr of CO_2. In the presence of ~600 Torr of CO_2, 2.74 ± 0.10 Torr of SO_2, and 2.74 ± 0.09 Torr of allene, [NO] was

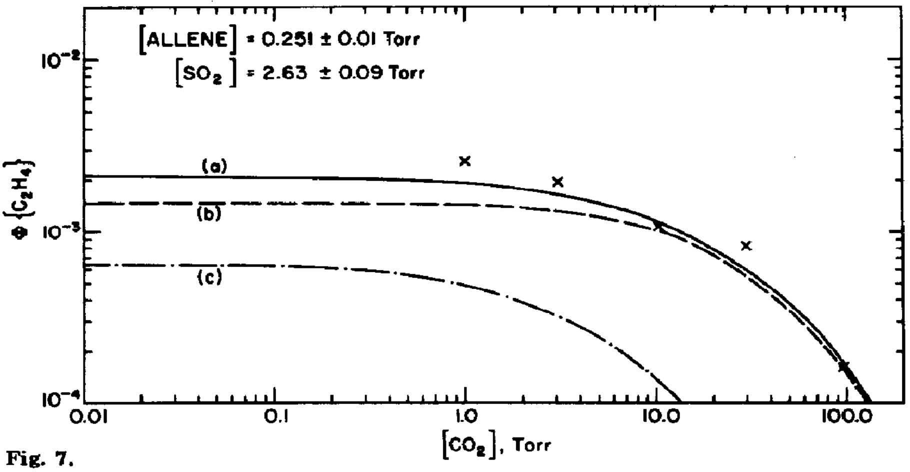

Fig. 7.

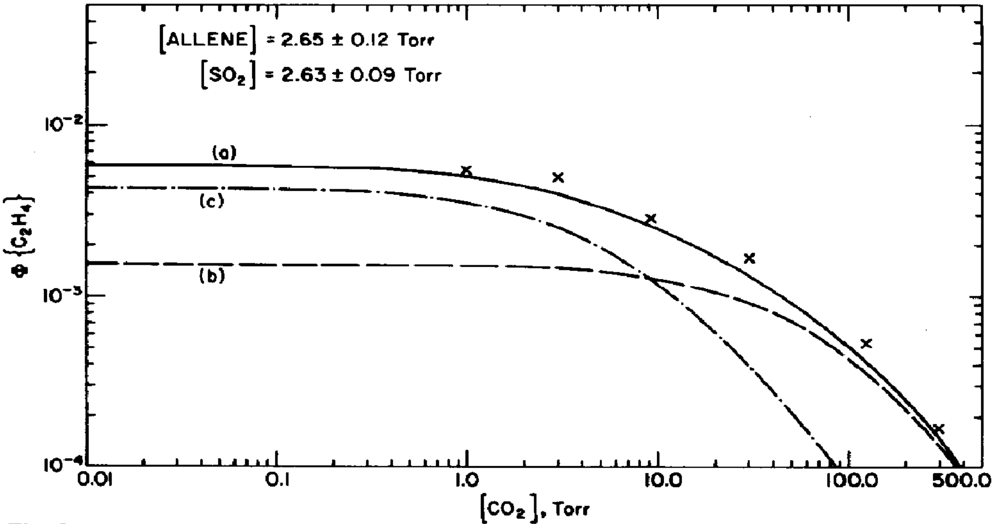

Fig. 8.

Figs. 7 and 8. Log–log plot of $\Phi\{C_2H_4\}$ *vs.* $[CO_2]$ for the photolysis of SO_2–allene mixtures in the presence of CO_2. The curves are theoretically computed from the rate coefficients listed in Table 1. (a), total $\Phi\{C_2H_4\}$; (b), $\Phi^3\{C_2H_4\}$; (c), $\Phi^1\{C_2H_4\}$.

varied from 76 mTorr to 145 Torr. $\Phi\{CO\}$, again the only measureable product, was quenched to a 50% value at approximately 4.0 Torr of NO (Fig. 25).

In the presence of ~600 Torr of CO_2, 2.75 ± 0.03 Torr of SO_2, and 2.75 ± 0.07 Torr of allene, $[H_2O]$ was varied from 1.19 to 18.2 Torr. $\Phi\{CO\}$ was found to be only slightly reduced by the addition of increasing amounts of H_2O (Fig. 26).

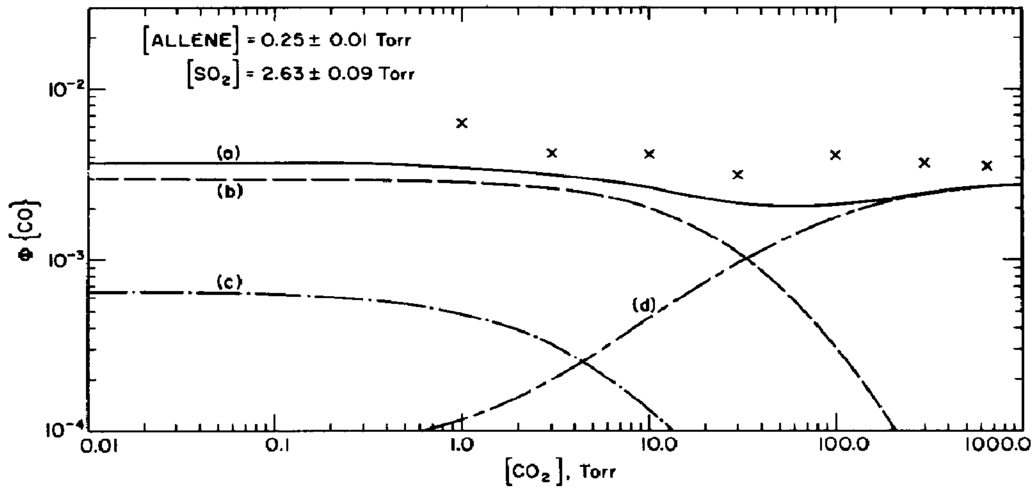

Fig. 9.

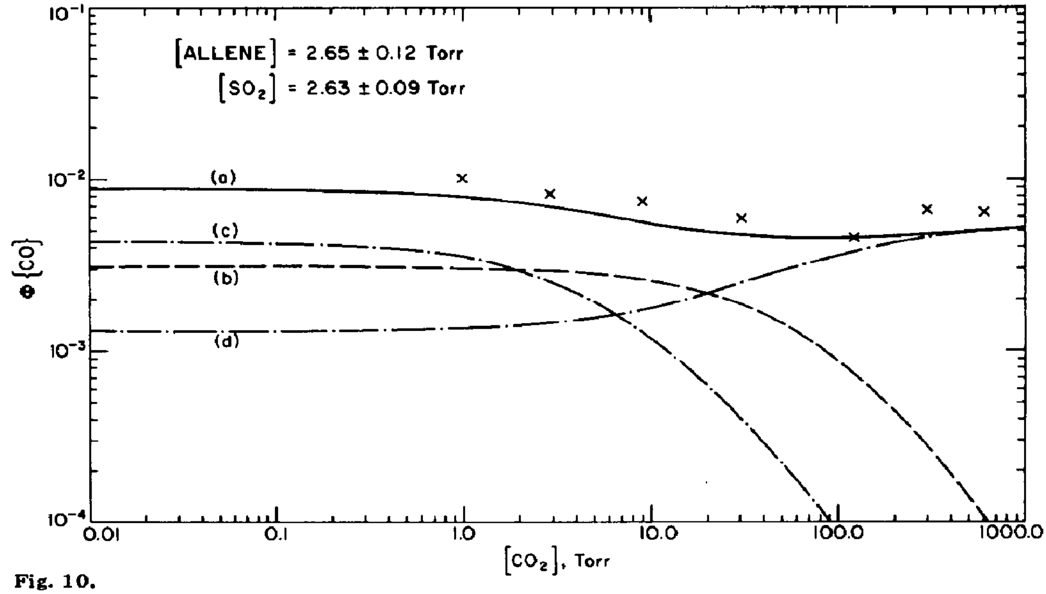

Fig. 10.

Figs. 9 and 10. Log-log plot of $\Phi\{CO\}$ *vs.* $[CO_2]$ for the photolysis of SO_2–allene mixtures in the presence of various pressures of CO_2. The curves are theoretically computed from the rate coefficients listed in Table 1. (a), total $\Phi\{CO\}$; (b), $\Phi^3\{CO\}$; (c), $\Phi^1\{CO\}$; (d), $\Phi^{**}\{CO\}$.

Discussion

The major conclusions that can be drawn from this study are:

(1) SO_2 photoexcited at 313.0 nm reacts with allene to produce CO, C_2H_4, and an aerosol.

(2) At the lowest [allene]/$[SO_2]$ ratios used in this study, the exclusive state involved in the chemistry in the $^3B_1$ state which emits phosphoresence.

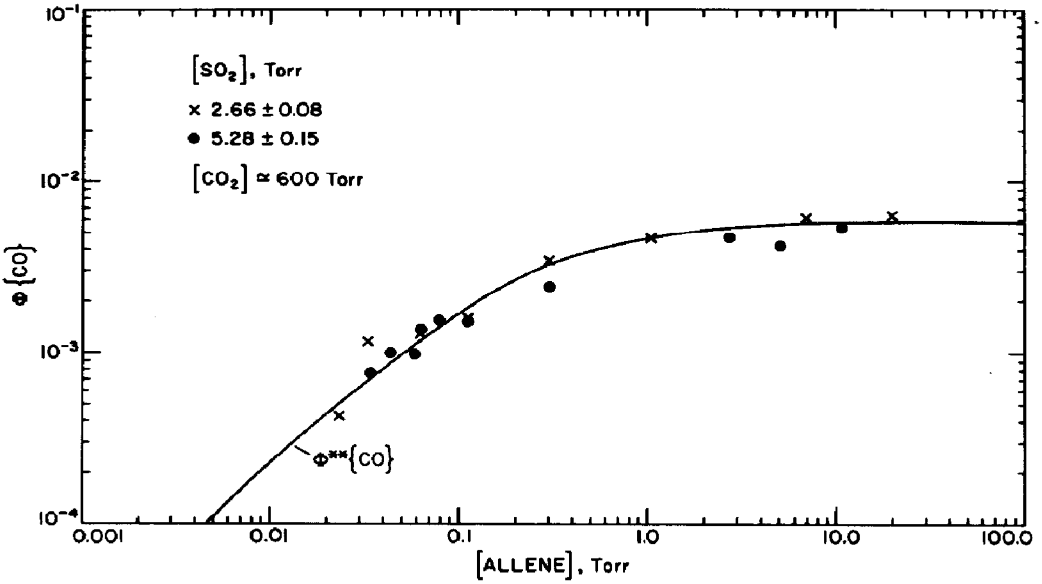

Fig. 11. Log–log plot of Φ{CO} *vs.* [allene] in the presence of ~600 Torr CO_2. Curve theoretically computed from rate coefficients in Table 1.

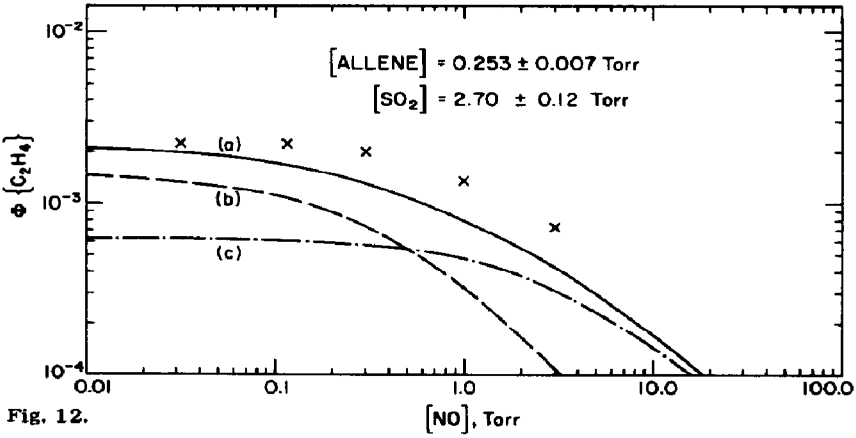

Fig. 12.

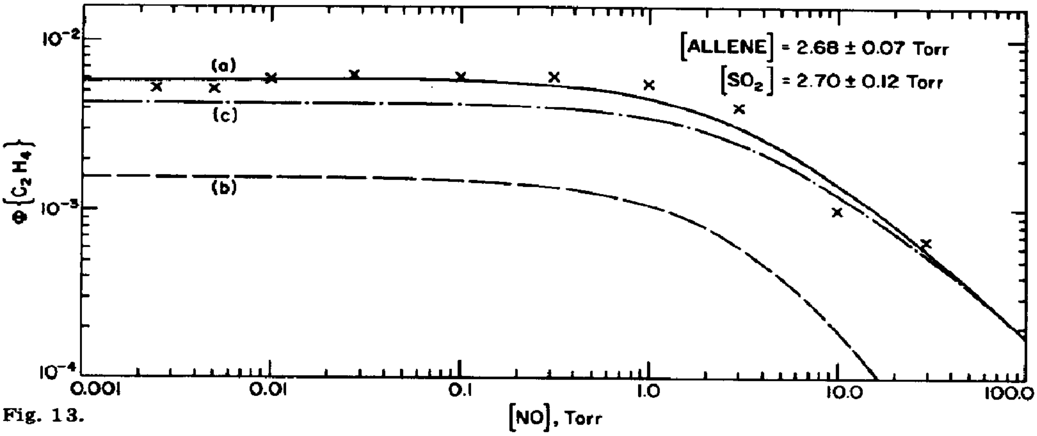

Fig. 13.

(For captions see overleaf.)

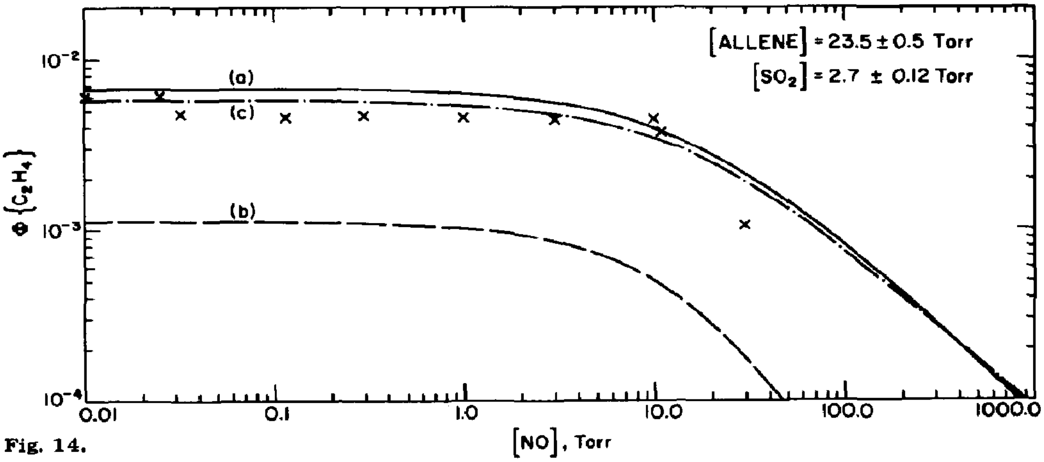

Fig. 14.

Figs. 12 - 14. Log–log plot of $\Phi\{C_2H_4\}$ vs. [NO] for the photolysis of SO_2–allene mixtures in the presence of NO. The curves are theoretically computed from the rate coefficients used in Table 1. (a), total $\Phi\{C_2H_4\}$; (b), $\Phi^3\{C_2H_4\}$; (c), $\Phi^1\{C_2H_4\}$.

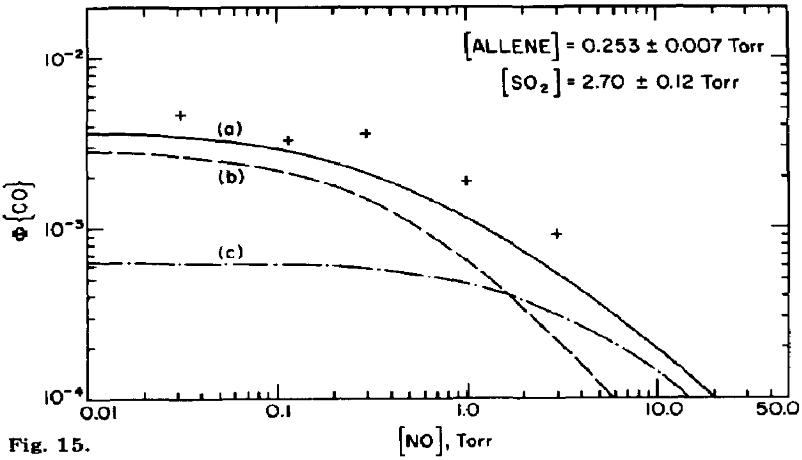

Fig. 15.

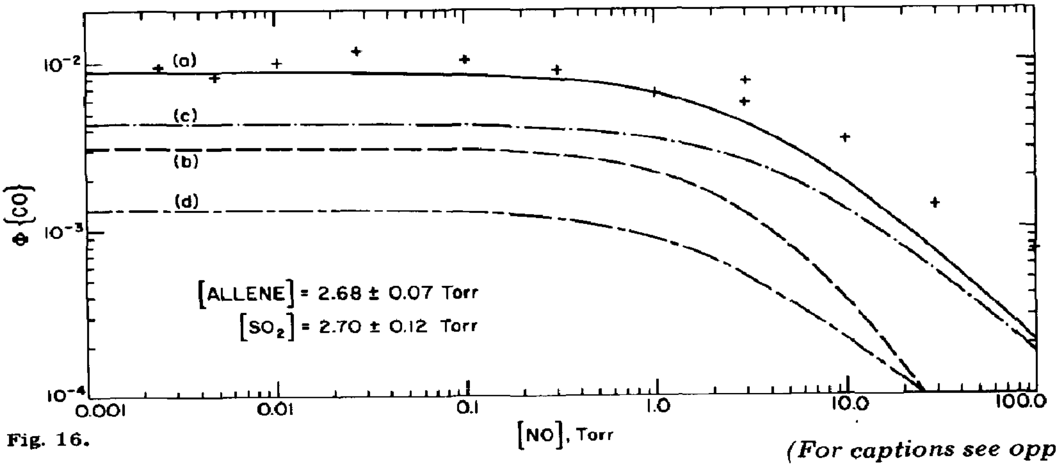

Fig. 16.

(For captions see opposite.)

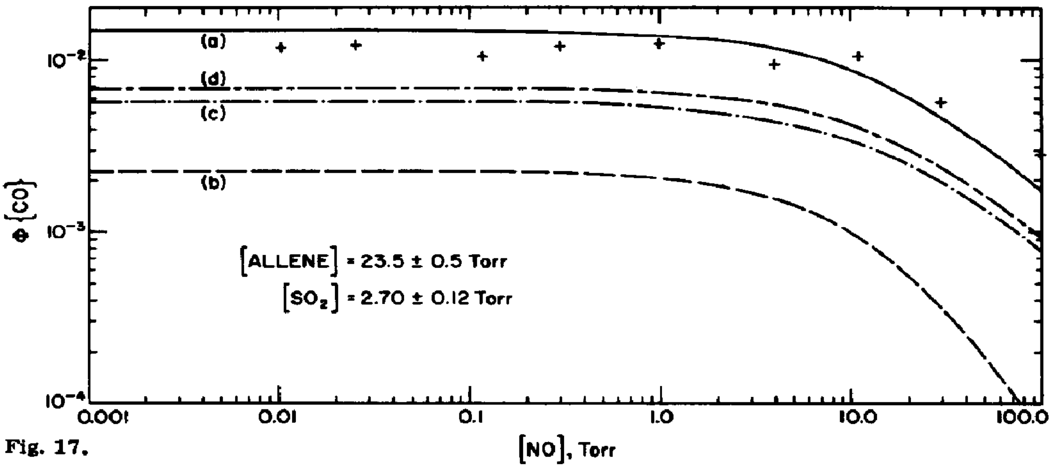

Fig. 17.

Figs. 15 - 17. Log–log plot of $\Phi\{CO\}$ *vs.* [NO] for the photolysis of SO_2–allene mixtures in the presence of NO. The curves are theoretically computed from the rate coefficients listed in Table 1. (a), total $\Phi\{CO\}$; (b), $\Phi^3\{CO\}$; (c), $\Phi^1\{CO\}$; (d), $\Phi^{**}\{CO\}$.

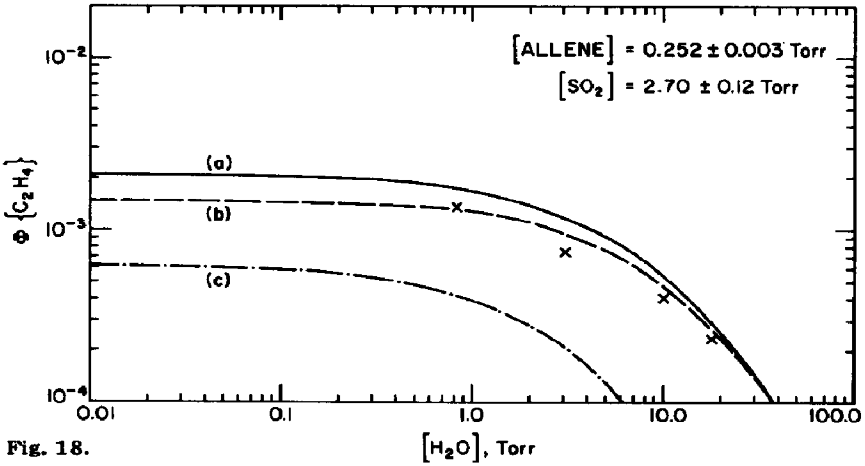

Fig. 18.

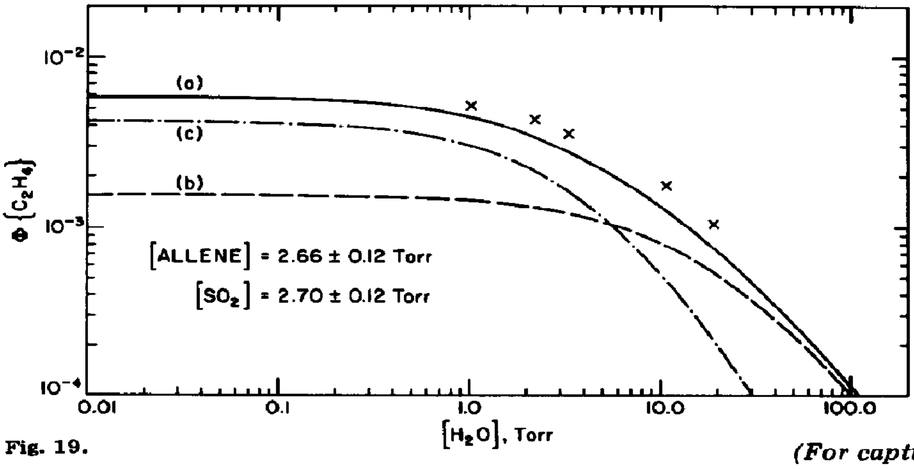

Fig. 19.

(For captions see overleaf.)

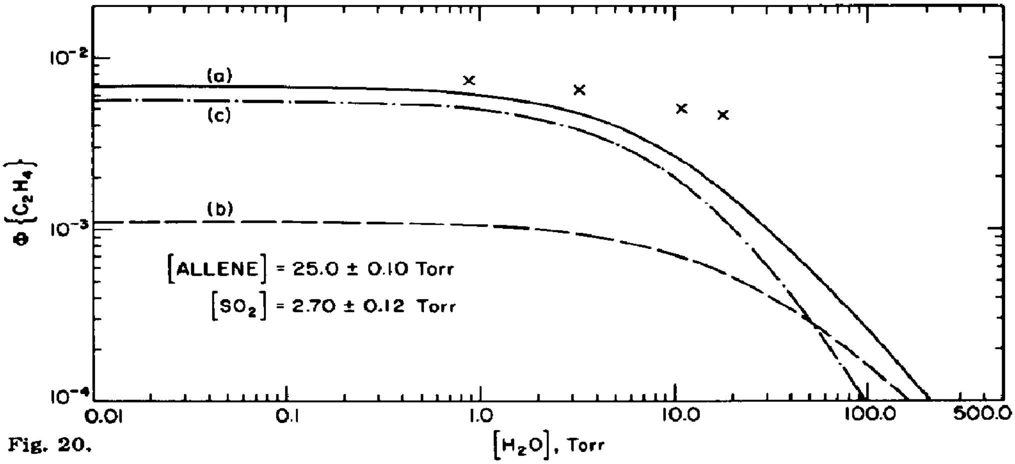

Fig. 20.

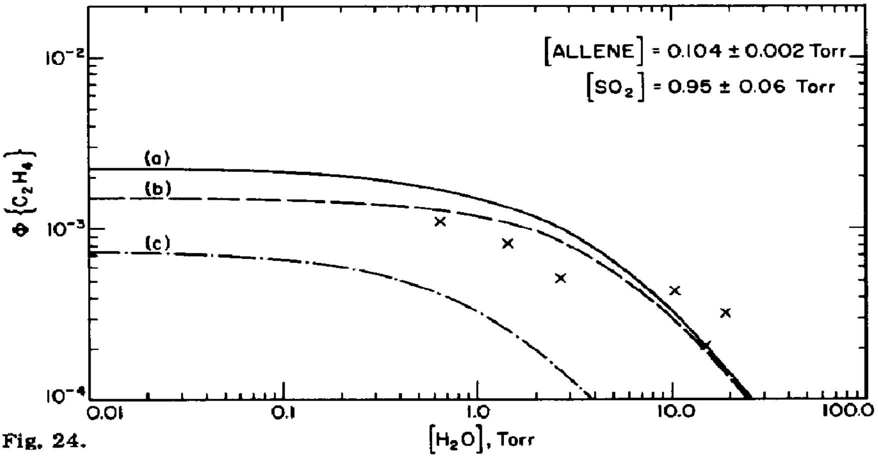

Fig. 24.

Figs. 18 - 20 and 24. Log–log plot of $\Phi\{C_2H_4\}$ *vs.* $[H_2O]$ for the photolysis of SO_2–allene mixtures in the presence of H_2O. The curves are theoretically computed from the rate coefficients listed in Table 1. (a), total $\Phi\{C_2H_4\}$; (b), $\Phi^3\{C_2H_4\}$; (c), $\Phi^1\{C_2H_4\}$.

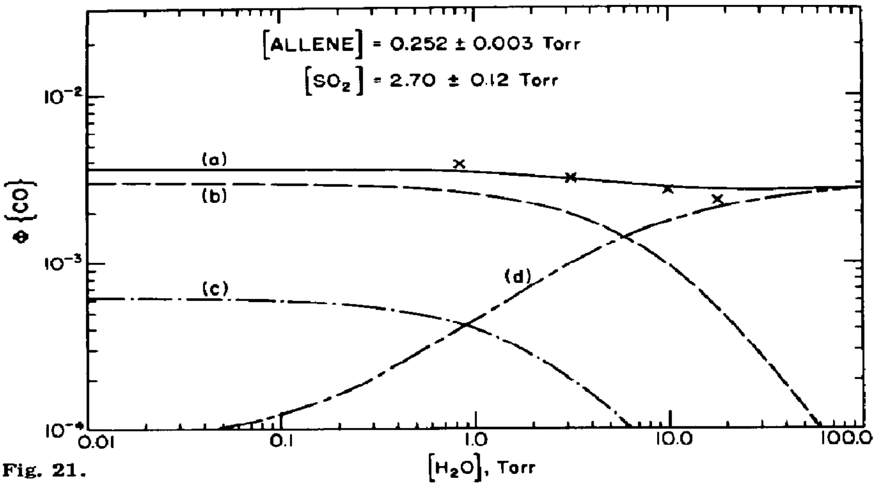

Fig. 21.

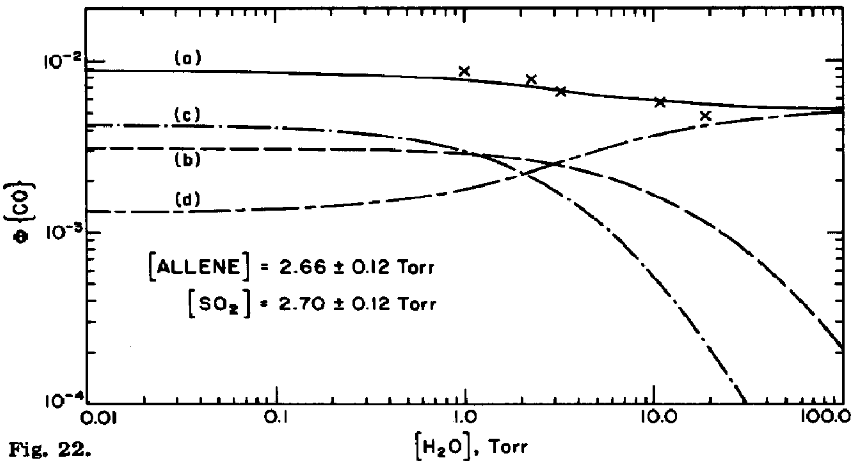

Fig. 22.

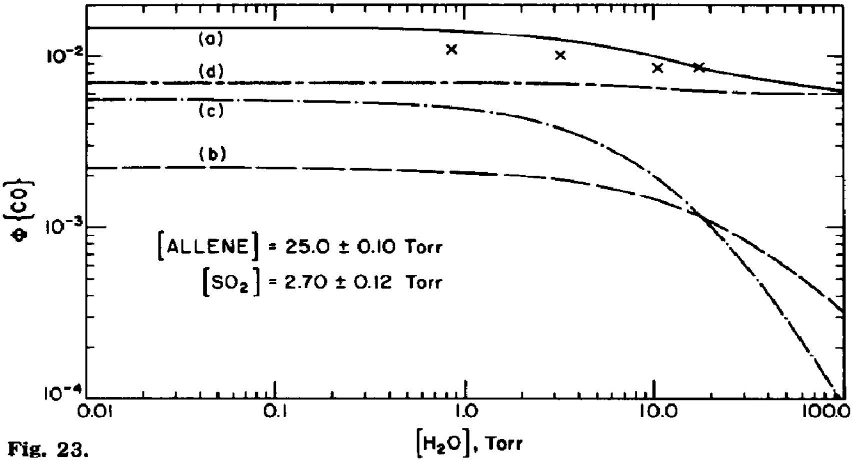

Fig. 23.

Figs. 21 - 23. Log–log plot of $\Phi\{CO\}$ *vs.* $[H_2O]$ for the photolysis of SO_2–allene mixtures in the presence of H_2O. The curves are theoretically computed from the rate coefficients listed in Table 1. (a), total $\Phi\{CO\}$; (b), $\Phi^3\{CO\}$; (c), $\Phi^1\{CO\}$; (d), $\Phi^{**}\{CO\}$.

This state is efficiently quenched by NO, an efficient triplet quencher, and its production depends only upon the ratio [allene] / $[SO_2]$, in accordance with our previous information on this state.

(3) The chemically reactive states include a singlet state as well as the triplet because product formation, though reduced, is not eliminated at higher values of the ratio [allene] / $[SO_2]$ when relatively large amounts of NO are added.

(4) The above two states are the only chemically reactive states which can lead to C_2H_4 production.

(5) A third chemically reactive triplet state, SO_2^{**}, which is not present at low pressures and is not quenched by SO_2, is also needed to produce CO but *not* C_2H_4. This is demonstrated experimentally by the fact that C_2H_4 is not produced in the presence of 600 Torr of CO_2, but CO is produced and $\Phi\{CO\}$ is independent of the SO_2 pressure (Fig. 11).

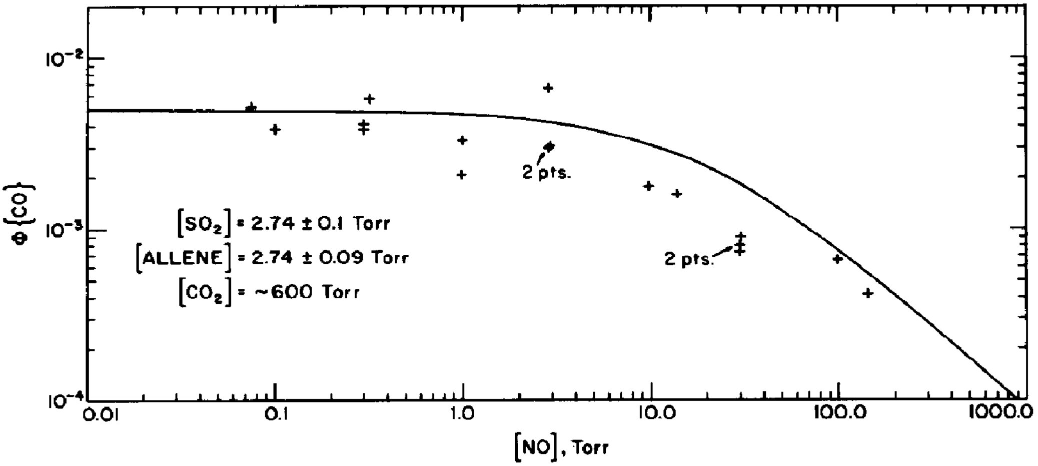

Fig. 25. Log–log plot of $\Phi\{CO\}$ *vs.* [NO] for the photolysis of SO_2–allene mixtures in the presence of NO and ~600 Torr of CO_2. The curve is theoretically computed from the rate coefficients in Table 1.

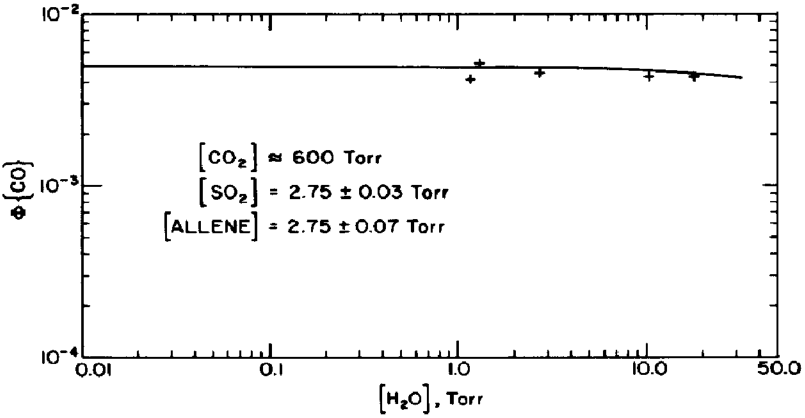

Fig. 26. Log–log plot of $\Phi\{CO\}$ *vs.* $[H_2O]$ for the photolysis of SO_2–allene mixtures in the presence of H_2O and ~600 Torr of CO_2. The curve is theoretically computed from the rate coefficients in Table 1.

The mechanism we have used to fit our results is one in which the major steps have been obtained from previous studies. A few new steps have been added to explain the uniqueness of the allene–SO_2 system. $SO_2(^3B_1)$ is abbreviated as $^3SO_2$, the fluorescing state as $^1SO_2$, the longer-lived of the two states formed by absorption as SO_2^*, and the non-emitting triplet state which is important at high pressure as SO_2^{**}. I symbolizes an intermediate postulated to form when $^3SO_2$ reacts with allene. It can unimolecularly decompose to give CO or C_2H_4 or it can be quenched, possibly to give the aerosol. All of the excited states and their quenching constants with SO_2, CO_2, NO, and H_2O have been established from previous studies. The intermediate I is a new species introduced here in order to fit the quenching data, which otherwise cannot be fitted. The entire mechanism proposed to explain this study is:

$$SO_2 + h\nu \xrightarrow{313\ \text{nm}} SO_2^* \qquad \text{Rate} = \alpha I_a$$

$$\xrightarrow{313\ \text{nm}} {}^3SO_2 \qquad \text{Rate} = \beta I_a$$

$$^3SO_2 \longrightarrow SO_2 + h\nu_p \tag{1}$$

$$^3SO_2 + \text{allene} \longrightarrow \text{I} \tag{2a}$$

$$\longrightarrow SO_2 + \text{allene} \tag{2b}$$

$$\text{I} \longrightarrow 2CO + C_2H_4 \tag{3}$$

$$\text{I} + \text{allene} \longrightarrow \text{not } CO \text{ or } C_2H_4 \tag{4a}$$

$$\text{I} + \text{M} \longrightarrow \text{not } CO \text{ or } C_2H_4 \tag{4b}$$

$$^3SO_2 + SO_2 \longrightarrow 2SO_2 \tag{5}$$

$$^3SO_2 + \text{M} \longrightarrow SO_2 + \text{M} \tag{6}$$

$$SO_2^* \longrightarrow {}^1SO_2 \tag{7a}$$

$$\longrightarrow SO_2 \tag{7b}$$

$$SO_2^* + \text{allene} \longrightarrow SO_2^{**} + \text{allene} \tag{8a}$$

$$\longrightarrow SO_2 + \text{allene} \tag{8b}$$

$$SO_2^* + \text{M} \longrightarrow SO_2^{**} + \text{M} \tag{9a}$$

$$\longrightarrow SO_2 + \text{M} \tag{9b}$$

$$^1SO_2 \longrightarrow SO_2 + h\nu_f \tag{10}$$

$$^1SO_2 + \text{allene} \longrightarrow C_2H_4 + CO \tag{11a}$$

$$\longrightarrow SO_2 + \text{allene} \tag{11b}$$

$$^1SO_2 + SO_2 \longrightarrow 2SO_2 \tag{12}$$

$$^1SO_2 + \text{M} \longrightarrow SO_2 + \text{M} \tag{13}$$

$$SO_2^{**} \longrightarrow SO_2 \tag{14}$$

$$SO_2^{**} + \text{allene} \longrightarrow CO \tag{15}$$

$$SO_2^{**} + NO \longrightarrow \text{not } CO \text{ or } C_2H_4 \tag{16}$$

where M is CO_2, NO, or H_2O.

The SO_2^* state is produced at a constant fraction, α, of the absorbed radiation intensity, I_a. It either forms $^1SO_2$ (discussed below) or unimolecularly decays. The SO_2^* state also can be collisionally deactivated to produce SO_2^{**} as well as ground state SO_2 but does not react to produce products. Cehelnik *et al.* [28] were the first to find that SO_2^{**} *must* come from this collisional quenching and *not* from a first-order process as this state is present only at high pressures where it is not quenched by SO_2, CO_2, or H_2O. The SO_2^{**} state is quenched by both allene and NO. The quenching by allene produces CO but not C_2H_4. It is not possible to evaluate whether SO_2^{**} is physically quenched by allene, so this reaction is omitted for simplicity.

$^3SO_2$ is produced at a constant fraction, β, of the absorbed radiation intensity I_a. This is not to imply that $^3SO_2$ *must* be produced directly on absorption but that whatever process of intersystem crossing which leads to it must be constant and thus pressure independent [37]. $^3SO_2$ might be produced from SO_2^* but this would necessitate a constant fraction of production by first order as well as collisional quenchings of SO_2^* by allene, CO_2, and H_2O because the Stern–Volmer quenching curve for $^3SO_2$ is linear [37]. It is very unlikely that these two removal processes would give $^3SO_2$ the same fraction of the time. Another possibility is that the $^3SO_2$ comes from the $^1A_2$ state which is collisionally deactivated at the pressures where this study was performed. The $^3SO_2$ state may be collisionally quenched by any gas present in the system and first-order removal steps are unimportant at the experimental pressures employed. The $^3SO_2$ is also postulated to react with allene to produce an excited intermediate state, I.

The proposed excited intermediate state, I, is formed by reaction of $^3SO_2$ with allene. It may then unimolecularly decompose to give CO and C_2H_4 in relative proportions of 2:1 via reaction (3). Reaction (3), of course, cannot proceed as written but represents two parallel paths of equal importance, one which produces CO + C_2H_4, and the other which produces CO but not C_2H_4. I may also be quenched by allene, CO_2, NO, and H_2O but not SO_2 (at the pressures used).

The longer-lived state formed by absorption of radiation is, presumably, $^1B_1$, but because of its non-linear Stern–Volmer quenching plot the state which fluoresces must be kinetically distinct and formed by a first-order process from SO_2^*, thus we designate it $^1SO_2$ [37]. From the viewpoint of photochemical kinetics it is immaterial whether this state is spectroscopically distinct or merely the result of a perturbation with the ground electronic state, as proposed by Brus and McDonald [34], because it behaves as a distinct entity. $^1SO_2$ may be collisionally quenched by any gas present in the system. First order removal of $^1SO_2$ is unimportant at the experimental pressures used. $^1SO_2$ reacts chemically with allene to form both CO and C_2H_4, presumably in equal proportions.

By a detailed analysis of the steady state expressions it is seen that:

$$\Phi\{C_2H_4\} = \frac{\beta k_{2a} k_3 [C_3H_4]}{(k_2[C_3H_4] + k_5[SO_2] + k_6[M])(k_3 + k_{4a}[C_3H_4] + k_{4b}[M])} + \frac{\alpha k_{7a} k_{11a} [C_3H_4]}{(k_7 + k_8[C_3H_4] + k_9[M])(k_{11}[C_3H_4] + k_{12}[SO_2] + k_{13}[M])} \tag{I}$$

and similarly:

$$\Phi\{CO\} = \frac{2\beta k_{2a} k_3 [C_3H_4]}{(k_2[C_3H_4] + k_5[SO_2] + k_6[M])(k_3 + k_{4a}[C_3H_4] + k_{4b}[M])} + \frac{\alpha k_{7a} k_{11a} [C_3H_4]}{(k_7 + k_8[C_3H_4] + k_9[M])(k_{11}[C_3H_4] + k_{12}[SO_2] + k_{13}[M])} +$$

$$+\frac{\alpha k_{15}[C_3H_4](k_{8a}[C_3H_4] + k_{9a}[M])}{(k_7 + k_8[C_3H_4] + k_9[M])(k_{14} + k_{15}[C_3H_4] + k_{16}[NO])} \qquad \text{(II)}$$

[M] in the above two equations represents [CO_2], [NO], or [H_2O]. The first term in each of the two equations represents the contribution to the quantum yield from the emitting triplet, $SO_2(^3B_1)$, state (via I) which will be referred to as $\Phi^3\{CO\}$ or $\Phi^3\{C_2H_4\}$. The second term in each equation is the contribution from the fluorescing singlet, $^1SO_2$, state and will be referred to as $\Phi^1\{CO\}$ or $\Phi^1\{C_2H_4\}$. The third term in the equation for $\Phi\{CO\}$ represents the contribution from SO_2^{**} and will be called $\Phi^{**}\{CO\}$. Thus eqns. (I) and (II) can be expressed as follows:

$$\Phi\{C_2H_4\} = \Phi^3\{C_2H_4\} + \Phi^1\{C_2H_4\} \qquad \text{(III)}$$

and

$$\Phi\{CO\} = \Phi^3\{CO\} + \Phi^1\{CO\} + \Phi^{**}\{CO\} \qquad \text{(IV)}$$

Analysis of C_2H_4 data, M gases absent

At values of [allene]/[SO_2] below 0.05, the first term in eqn. (I) is predominant. In the absence of foreign gases, eqn. (I) can be rearranged to:

$$\Phi\{C_2H_4\}^{-1} = \frac{k_2}{\beta k_{2a}}\left(1 + \frac{k_5[SO_2]}{k_2[C_3H_4]}\right)\left(1 + \frac{k_{4a}[C_3H_4]}{k_3}\right) \qquad \text{(V)}$$

Figure 27 is a plot of $\Phi\{C_2H_4\}^{-1}$ *vs.* [SO_2]/[C_3H_4]. The data are scattered,

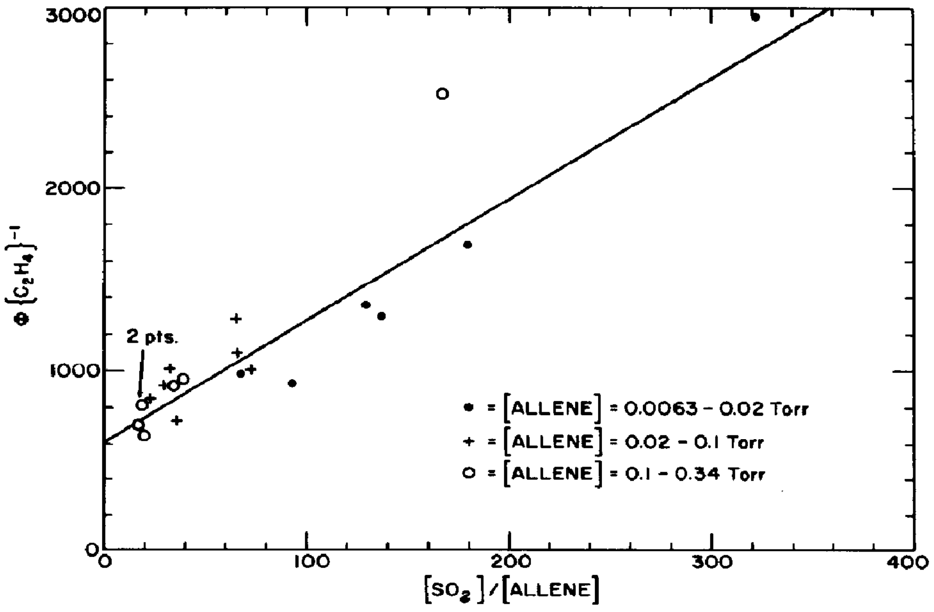

Fig. 27. Plot of the reciprocal of the C_2H_4 quantum yield *vs.* [SO_2]/[allene] for values of [allene]/[SO_2] below 0.05.

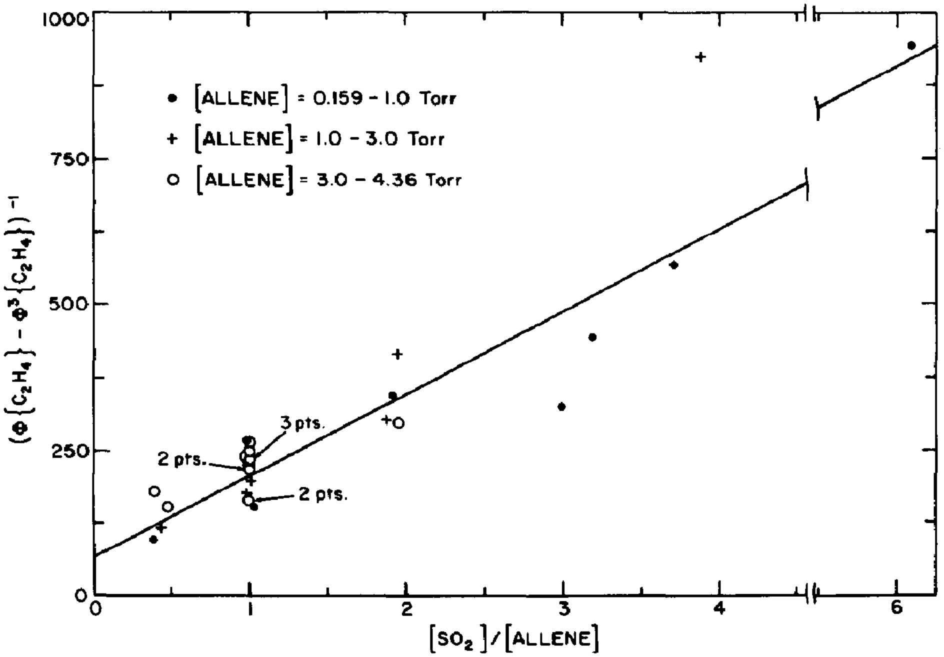

Fig. 28. Plot of the reciprocal of ($\Phi\{C_2H_4\} - \Phi^3\{C_2H_4\}$) *vs.* $[SO_2]/[\text{allene}]$ at intermediate values of $[\text{allene}]/[SO_2]$.

but there is no evidence of a dependence other than on the ratio, *i.e.* the results at different C_3H_4 pressures but the same value of $[SO_2]/[C_3H_4]$ are the same. Thus $k_{4a}[C_3H_4]/k_3 \ll 1$. The data are fitted by the best straight line. The intercept gives $k_2/\beta k_{2a} = 600$ and the ratio of intercept to slope gives $k_2/k_5 = 90$. The values of β have been given by Demerjian and Calvert [17] ; and at 313.0 nm, it has been found to have a value of approximately 0.10. Thus $k_{2a}/k_2 = 0.0167$. These values are summarized in Table 1.

In the absence of foreign gases at higher values of [allene]/$[SO_2]$, where $\Phi\{C_2H_4\}$ is still increasing with [allene]/$[SO_2]$, it is possible to evaluate the second term on the right-hand side of eqn. (I) by a plot of $1/(\Phi\{C_2H_4\} - \Phi^3\{C_2H_4\})$ *versus* $[SO_2]/[\text{allene}]$, since:

$$1/(\Phi\{C_2H_4\} - \Phi^3\{C_2H_4\}) = \frac{k_7 k_{11}}{\alpha k_{7a} k_{11a}}\left(1 + \frac{k_{12}[SO_2]}{k_{11}[C_3H_4]}\right)\left(1 + \frac{k_8[C_3H_4]}{k_7}\right) \quad \text{(VI)}$$

The values for $\Phi^3\{C_2H_4\}$ are computed from the rate coefficient ratios determined above, and the left-hand side of eqn. (VI) is plotted *vs.* $[SO_2]/[C_3H_4]$ in Fig. 28. Again there is a large scatter in the data but no noticeable dependence on $[C_3H_4]$ other than through the ratio $[SO_2]/[C_3H_4]$. Consequently $k_8[C_3H_4]/k_7 \ll 1$ and the data are fitted by a straight line. From the intercept, $k_7 k_{11}/\alpha k_{7a} k_{11a} = 68$; and from the ratio of intercept to slope, $k_{11}/k_{12} = 0.49$.

At the highest values of [allene]/$[SO_2]$, which also corresponds to high allene pressures, the term $k_{12}[SO_2]/k_{11}[C_3H_4]$ in eqn. (VI) becomes negligible, and the rate law reduces to:

TABLE 1

Summary of rate coefficient data

Ratio	Value	Units	M	Reference
β	0.10	None	—	Demerjian and Calvert [17]
$\alpha = 1 - \beta$	0.90	None	—	Demerjian and Calvert [17]
k_2/k_5	90	None	C_3H_4	This work
k_{2a}/k_2	0.0167	None	C_3H_4	This work
k_{4a}/k_3	0.02	$Torr^{-1}$	C_3H_4	This work
k_{4b}/k_3	0.02	$Torr^{-1}$	CO_2	This work
	0.1	$Torr^{-1}$	NO	This work
	0.08	$Torr^{-1}$	H_2O	This work
k_6/k_5	0.55	None	CO_2	This work
	0.42	None	CO_2	Kelly *et al.* [18]
	0.31	None	CO_2	Mettee [10]
	0.55	None	CO_2	Stockburger *et al.* [37]
	0.29	None	CO_2	Sidebottom *et al.* [27]
k_6/k_5	80	None	NO	This work
	80	None	NO	Kelly *et al.* [18]
	64	None	NO	Mettee [10]
	~100	None	NO	Stockburger *et al.* [37]
	190	None	NO	Sidebottom *et al.* [27]
k_6/k_5	1.80	None	H_2O	This work
	1.62	None	H_2O	Kelly *et al.* [18]
	1.8	None	H_2O	Stockburger *et al.* [37]
	2.28	None	H_2O	Sidebottom *et al.* [27]
k_7/k_8	22	Torr	C_3H_4	This work
k_9/k_7	0.015	$Torr^{-1}$	CO_2	This work
	0.0179	$Torr^{-1}$	CO_2	Kelly *et al.* [18]
	~0.025	$Torr^{-1}$	CO_2	Stockburger *et al.* [37]
k_9/k_7	0.15	$Torr^{-1}$	H_2O	This work
	0.23	$Torr^{-1}$	H_2O	Kelly *et al.* [18]
	~0.1	$Torr^{-1}$	H_2O	Stockburger *et al.* [37]
$k_7k_{11}/\alpha k_{7a}k_{11a}$	68	None	C_3H_4	This work
k_{11}/k_{12}	0.49	None	C_3H_4	This work
k_{13}/k_{12}	0.85	None	CO_2	This work
	0.76	None	CO_2	Stockburger *et al.* [37]
	0.63	None	CO_2	Mettee [10]
	0.73	None	CO_2	Rao *et al.* [14]
k_{13}/k_{12}	0.94	None	NO	This work
	0.86	None	NO	Stockburger *et al.* [37]
	0.59	None	NO	Mettee [10]
k_{13}/k_{12}	1.01	None	H_2O	This work
	0.93	None	H_2O	Stockburger *et al.* [37]
k_{14}/k_{15}	0.255	Torr	C_3H_4	This work
k_{14}/k_{16}	0.17	Torr	NO	This work
	0.164	Torr	NO	Kelly *et al.* [18]
	0.34	Torr	—	Cehelnik *et al.* [28]
$k_9/\alpha k_{9a}$	170	None	CO_2	This work
	45.2	None	CO_2	Kelly *et al.* [18]

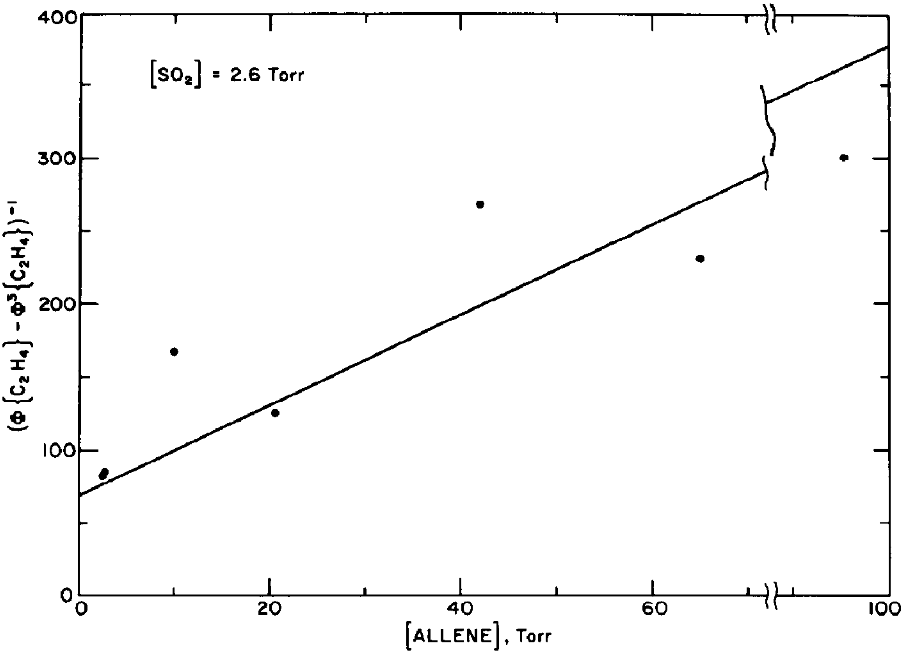

Fig. 29. Plot of the reciprocal of $(\Phi\{C_2H_4\} - \Phi^3\{C_2H_4\})$ *vs.* [allene] at allene pressures greater than 2.6 Torr.

$$1/(\Phi\{C_2H_4\} - \Phi^3\{C_2H_4\}) = \frac{k_7 k_{11}}{\alpha k_{7a} k_{11a}}(1 + k_8[C_3H_4]/k_7) \qquad \text{(VII)}$$

Figure 29 is a plot of $1/(\Phi\{C_2H_4\} - \Phi^3\{C_2H_4\})$ *versus* [allene], and the data points can be fitted by a straight line. The intercept gives $k_7k_{11}/\alpha k_{7a}k_{11a}$ = 68, consistent with the value obtained from Fig. 28. The ratio of intercept to slope gives k_7/k_8 = 22 Torr. (This is an approximation because $\Phi^3\{C_2H_4\}$ is slightly quenched by allene also. Within the experimental uncertainty of the data, however, the correction is of no consequence.)

Analysis of C_2H_4 data, M gases present

In no pressure regime where it was possible to perform experiments and obtain sufficient product yields for analysis was it also possible to uncouple the reactions of $^1SO_2$ and $^3SO_2$ with allene to produce C_2H_4 or CO. Therefore the quenching experiments performed with CO_2, NO, and H_2O were analyzed on the basis of the quenching data of others in this laboratory [18, 28, 37] and elsewhere [4, 10, 27]. Initially the intermediate I was omitted and it was assumed that reaction (2a) gave C_2H_4 directly. It was apparent that the extent of quenching computed from the known rate coefficient ratios was less than actually observed. Thus the intermediate I was introduced, and the data in Figs. 7, 8, 12 - 14, and 18 - 20 were computer fitted. The best fit was obtained with the rate coefficient ratios listed in Table 1, most of which are averages or "best values" from previous investigations. The only entirely new rate coefficient ratios from this work

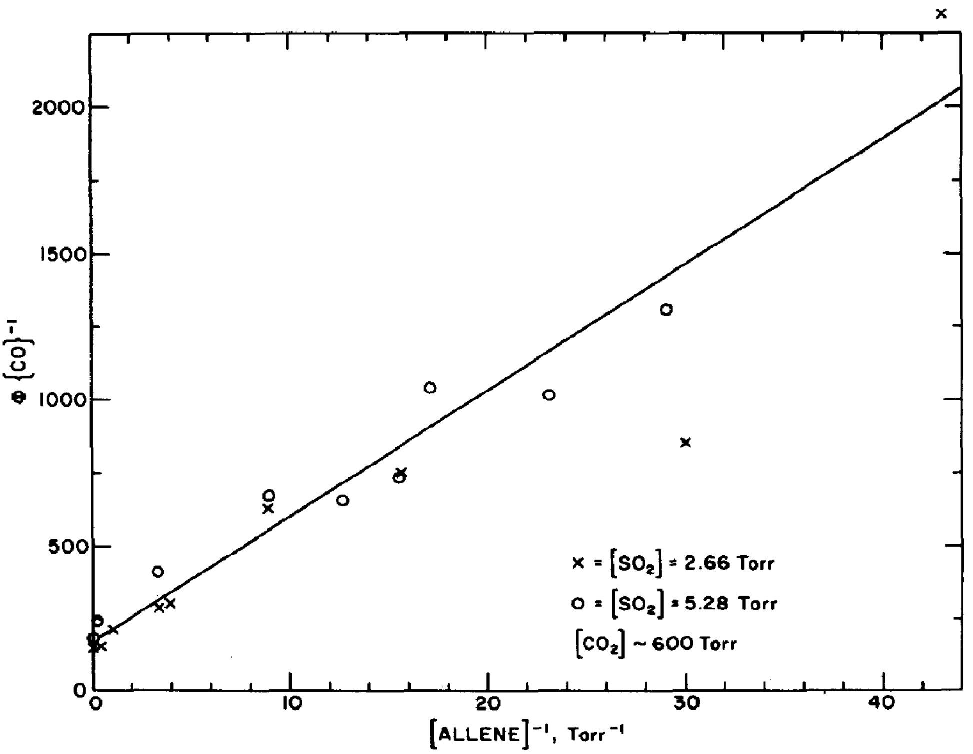

Fig. 30. Plot of the reciprocal of the CO quantum yield *vs.* the reciprocal allene pressure for the photolysis of SO_2–allene mixtures in the presence of ~600 Torr of CO_2.

are k_{4a}/k_3 and k_{4b}/k_3. The computed curve for $\Phi\,\{C_2H_4\}$ is given by the curve (a) in each of the Figures, and the data are reasonably well fitted.

Analysis of CO data, 600 Torr CO_2 present

In the presence of 600 Torr of CO_2 and at low allene pressures the first two contributions to $\Phi\,\{CO\}$ in eqn. (II) are completely quenched. What is left is the high pressure, SO_2^{**}, state discovered by Cehelnik *et al.* [28] and since reported by others [28 - 31, 37]. Furthermore reaction (8) is negligible compared to reaction (9). Thus eqn. (II) reduces to:

$$\Phi\,\{CO\}^{-1} = \Phi^{**}\,\{CO\}^{-1} = \frac{k_9}{\alpha k_{9a}}\left(1 + \frac{k_{14}}{k_{15}[C_3H_4]}\right) \qquad \text{(VIII)}$$

A plot of $\Phi\,\{CO\}^{-1}$ *vs.* $[\text{allene}]^{-1}$ is shown in Fig. 30. The data can be fitted by a straight line whose intercept gives $k_9/\alpha k_{9a} = 170$ and whose slope gives $k_{14}/k_{15} = 0.255$ Torr. The value for $k_9/\alpha k_{9a} = 170$ is considerably different than that of 45.2 obtained by Kelly *et al.* [18]. This apparent discrepancy results from a simplification in the mechanism since we have assumed that removal of SO_2^{**} by allene (or C_2H_2 in the study of Kelly *et al.*) always produces products. If deactivation of SO_2^{**} by physical quenching with allene occurs ~80% of the time, then the discrepancy is resolved.

Analysis of CO data, M gases absent

Now it is possible to compare the experimental values of $\Phi\{CO\}$ (Figs. 2 - 6) with those obtained from the various contributions of $^1SO_2$, $^3SO_2$, and SO_2^{**}. This was done initially assuming that CO and C_2H_4 were produced in equal amounts from both $^1SO_2$ and $^3SO_2$. It was seen that there was a discrepancy in the predicted values which was equal to the contribution expected from $^3SO_2$ and thus it is hypothesized that two CO molecules are produced for every one C_2H_4 molecule formed in reaction (3). This means that I represents two intermediates (or the same intermediate with different amounts of vibrational energy) and that reaction (3) actually represents (2) reactions:

$$\mathrm{I} \longrightarrow \mathrm{CO} + \mathrm{C_2H_4}\ (+\ \mathrm{SO}) \tag{3a}$$

$$\mathrm{I} \longrightarrow \mathrm{CO}\ (+\ \mathrm{C_2H_4SO}) \tag{3b}$$

The computed curves for $\Phi\{CO\}$ are shown in Figs. 2 - 6. In some cases they lie somewhat below the data points, but the trends are all reproduced.

Analysis of CO data, M gases present

$\Phi\{CO\}$ data obtained at various ratios of [allene]/[SO_2] in the presence of varying amounts of CO_2, NO, and H_2O can be closely approximated by using the rate constant ratios previously derived in this study as well as several quenching rate constant ratios, as mentioned earlier, which were taken from the work of others and computing them from eqn. (II). The computed values agree well with the data (Figs. 9 - 11, 15 - 17, and 21 - 23). Two series of experiments were performed by adding various amounts of either NO or H_2O to reaction mixtures of allene and SO_2 containing 600 Torr of CO_2. Values of $\Phi\{CO\}$ computed from the proposed rate coefficient ratios predict quenching plots which approximate these data very well (Figs. 25 and 26).

Conclusions

The SO_2–allene system is complex in that it involves contributions from several excited states of SO_2 as well as a proposed excited intermediate state. The mechanism proposed is an attempt to simplify as well as to approximate the major features of this system. The rate coefficient ratios deduced from this study have been used to compute the expected quantum yields. These computed curves, along with the contributions from the individual excited state of SO_2, are shown in Figs. 1 - 26. As can be seen from the predicted quantum yield plots this mechanism is generally successful to within the limits of the experimental uncertainty. Many of the rate constants derived are unique to this study and represent what would be considered to be reasonable values from what is known about allene and the other gases used and their relative reactivities. In the cases where comparison can be made with the data of others, our experimental results agree well with these data. Most importantly, this study once again demonstrates that the emitting states of photoexcited SO_2 are not always sufficient to explain the data. The SO_2^{**} state which occurs only at high pressures has once again been shown to exist and play an important role in SO_2 photochemistry.

Acknowledgements

We wish to thank Mr. Nelson Kelly and Dr. Leonard Stockburger, III for helpful discussions. This work was supported by the Center for Air Environment Studies at Penn State University for which we are grateful.

References

1 H. D. Mettee, J. Chem. Phys., 49 (1968) 1784.
2 S. J. Strickler and D. B. Howell, J. Chem. Phys., 49 (1968) 1947.
3 T. N. Rao, S. S. Collier and J. G. Calvert, J. Am. Chem. Soc., 91 (1969) 1609.
4 T. N. Rao, S. S. Collier and J. G. Calvert, J. Am. Chem. Soc., 91 (1969) 1616.
5 K. F. Greenough and A. B. F. Duncan, J. Am. Chem. Soc., 83 (1961) 555.
6 R. B. Caton and A. B. F. Duncan, J. Am. Chem. Soc., 90 (1968) 1945.
7 H. D. Mettee, J. Am. Chem. Soc., 90 (1968) 2972.
8 S. Okuda, T. N. Rao, D. H. Slater and J. G. Calvert, J. Phys. Chem., 73 (1969) 4412.
9 S. S. Collier, A. Morikawa, D. H. Slater, J. G. Calvert, G. Reinhardt and E. Damon, J. Am. Chem. Soc., 92 (1970) 217.
10 H. D. Mettee, J. Phys. Chem., 73 (1969) 1071.
11 F. S. Dainton and K. T. Ivin, Trans. Faraday Soc., 46 (1950) 374.
12 F. S. Dainton and K. T. Ivin, Trans. Faraday Soc., 46 (1950) 382.
13 R. B. Timmons, Photochem. Photobiol., 12 (1970) 219.
14 F. B. Wampler, A. Horowitz and J. G. Calvert, J. Am. Chem. Soc., 94 (1972) 5523.
15 R. A. Cox, J. Photochem., 2 (1973/74) 1.
16 R. D. Penzhorn and G. H. Gusten, Z. Naturforsch., 27a (1972) 1401.
17 K. L. Demerjian and J. G. Calvert, Int. J. Chem. Kinet., 7 (1975) 45.
18 N. Kelly, J. F. Meagher, and J. Heicklen, J. Photochem., 5 (1976) 355.
19 G. E. Jackson and J. G. Calvert, J. Am. Chem. Soc., 93 (1971) 2593.
20 C. C. Badcock, H. W. Sidebottom, J. G. Calvert, G. W. Reinhardt and E. K. Damon, J. Am. Chem. Soc., 93 (1971) 3115.
21 K. L. Demerjian, J. G. Calvert and D. L. Thorsell, Int. J. Chem. Kinet., 6 (1974) 829.
22 H. W. Sidebottom, C. C. Badcock, J. G. Calvert, B. R. Rabe and E. K. Damon, J. Am. Chem. Soc., 93 (1971) 3121.
23 F. B. Wampler, Int. J. Chem. Kinet., 8 (1976) 511.
24 F. B. Wampler and J. W. Bottenheim, Kinet., 8 (1976) 585.
25 F. B. Wampler, Int. J. Chem. Kinet., 8 (1976) 687.
26 N. Kelly, J. F. Meagher and J. Heicklen, J. Photochem., 6 (1976/77) 157.
27 H. W. Sidebottom, C. C. Badcock, G. E. Jackson, J. G. Calvert, G. W. Reinhardt and E. K. Damon, Environ. Sci. Technol., 6 (1972) 72.
28 E. Cehelnik, C. W. Spicer and J. Heicklen, J. Am. Chem. Soc., 93 (1971) 5371.
29 E. Cehelnik, J. Heicklen, S. Braslavsky, L. Stockburger, III and E. Mathias, J. Photochem., 2 (1973) 31.
30 S. Braslavsky and J. Heicklen, J. Am. Chem. Soc., 94 (1972) 4864.
31 A. M. Fatta, E. Mathias, J. Heicklen, L. Stockburger, III and S. Braslavsky, J. Photochem., 2 (1973) 119.

32 R. D. Penzhorn and W. G. Filby, J. Photochem., 4 (1975) 91.
33 K. Chung, J. G. Calvert and J. W. Bottenheim, Int. J. Chem. Kinet., 7 (1975) 161.
34 L. E. Brus and J. R. McDonald, Chem. Phys. Lett., 21 (1973) 283; J. Chem. Phys., 61 (1974) 97.
35 F. C. James, J. A. Kerr and J. P. Simons, Chem. Phys. Lett., 25 (1974) 431.
36 F. B. Wampler, J. G. Calvert and E. K. Damon, Int. J. Chem. Kinet., 5 (1973) 107.
37 L. Stockburger, III, S. Braslavsky and J. Heicklen, J. Photochem., 2 (1973) 15.
38 M. Luria and J. Heicklen, Can. J. Chem., 52 (1974) 3451.
39 M. Luria, R. G. de Pena, K. J. Olszyna and J. Heicklen, J. Aerosol Sci., 5 (1974) 435.
40 R. Renaud and L. C. Leitch, Can. J. Chem., 32 (1954) 549.
41 F. W. Williams, F. J. Woods and M. E. Umstead, J. Chromat. Sci., 10 (1972) 570.